Direct Excitations of He$^+$ and Li^{++} Ions by Collisions with Protons or Antiprotons

Reda S. Tantawi[1] and T. E. I. Nassar[2]

[1] Mathematics Department, Faculty of Science, Zagazig University, Zagazig, Egypt.

[2] Department of Basic Science, Higher Technological Institute, 10th of Ramadan City, Egypt.

E. mails: reda_tantawi2@yahoo.com

Abstract: The impact parameter formalism of the single-center close-coupling, first-, and second-order Born approximations have been applied to investigate direct excitations of Helium He$^+$(2s) and Lithium Li^{++}(2s) ions by colliding with protons or antiprotons. The total 3s, 3p, and 3d scaled excitation cross sections are calculated in the scaled impact energy region (2 to 1000 keV). The present work aims to explore the sensitivity of the cross sections to the different electronic transition mechanisms of the considered approaches as well as the charge of each of the projectile and the target nucleus. Also, the calculated cross sections are compared with those obtained by previous theoretical calculations.

1. Introduction

The ion collision process is an important topic in atomic and molecular physics. Detailed knowledge of excitation and ionization processes of such collisions is of both fundamental importance of our understanding of quantum scattering theories and of practical importance to fields like astrophysics, laser physics, fusion and plasma physics. Electronic transitions in protons or antiprotons impacts on one-electron ions are fundamental atomic collision processes and can be treated with considerable accuracy. In such collisions, as the charge of the target nucleus increases the interaction between the projectile and the electron of the ion in the process of excitation becomes much weaker than the interaction between the electron and the ionic nucleus. Therefore, it can be regarded as a weak perturbation.

Collisions with antiprotons are different from that with protons in their capture behavior. Electron capture by proton projectile is possible at low impact energies [1]. On the other side, the antiproton projectile can annihilate with the proton of the target nucleus. The annihilation process is likely to occur at very low collision energies [2].

While various theoretical methods have been used from time to time to investigate excitation processes induced by proton (antiproton) collisions with one-electron atoms, the close-coupling ones show great success in such processes [3-5] and have been proven to be the workhorse for the prediction of experimental results over a broad range of energies. In the framework of the first-order Born approximation, the results for matter and antimatter scattering process are the same and are of reasonably accurate at high collision energies [6-8].

In the single-center close-coupling method [9, 10], an expansion of basis functions around the target nucleus only is employed and no electron translation factor is necessary because the expansion satisfies the correct scattering boundary conditions. It is appropriate to employ the single-center close-coupling approach for collisions that cause predominantly direct excitations or involve antiproton projectiles.

Even the collisions of protons or antiprotons with ground-state hydrogenlike ions are the subject of many investigations [11-19], there are limited calculations on the collision processes involving initial excited-state hydrogenlike target ions.

A single-center expansion method has been used to study excitation of Helium He^+ ion, being initially in the excited 2s or 2p states, by protons impact [11]. The wavefunction of the system is represented in the interaction picture, and the transition amplitudes are calculated by using a time-development operator for which the basis states are the matrix eigenvectors of the target Hamiltonian and are obtained by diagonalizing that Hamiltonian on an underlying basis. Similar calculations are performed for the excitation of Lithium Li++ ion in the collision with proton [12].

Liu et al. [20] used the two-center atomic orbital close-coupling method to investigate the dynamics of excitation and electron-capture processes in the He^{++} + He^+(2s) collision system with screened Coulomb interactions of a Debye-Huckel potential type. Gusarevich et al. [21] used the relativistic eikonal approximation and a matching procedure to describe excitation and ionization of hydrogenlike atoms from an arbitrary discrete energy state by the impact of a highly charged relativistic bare ion. Bethe-type formulas were derived that are asymptotically valid in the limits that the relative collision velocity approaches the speed of the light and high ion charge.

Tantaw [22] presented coupled-state excitation cross sections of hydrogelike ions H, He$^+$ and Li^{++}, being initially in the 2s state by proton and antiproton impacts. The calculations considered couplings between n = 1, 2, 3, and 4 states of the target ions only. It was found that, increasing the charge of the target nucleus enhance the effect of the sign of the projectile charge. The effect of the charge of the target nucleus in proton-induced reactions was found to be greater than it was in the reactions of antiprotons. Similar calculations but allowing couplings to and between n= 1- 5 states of the target ion are achieved for excitations of hydrogenlike ions H(2p), He$^+$(2p) and Li^{++}(2p) by proton and antiproton impacts [23]. It was found that the cross sections are strongly affected by neglecting the back-coupling matrix potential elements and are weakly affected by neglecting the 2s-2p couplings.

Recently, Tantawi and Nagah [24] demonstrated calculations for n=3 excitation cross sections of H(2s) atoms by protons and antiprotons impact. The calculations are based on a close-coupling approximation as well as the impact parameter versions of the first- and second-order Born approximations.

In the present work we extend the work of Ref. [24] to investigate scaled cross sections for direct excitations of Helium He$^+$(2s) and Lithium Li^{++}(2s) ions by protons or antiprotons impacts. We aim to explore the effect of the charge of each of the projectile and the ionic nucleus besides the electronic transition mechanisms allowed by the approximations under consideration on the calculated scaled cross sections.

2. Formulation of the problem

In ion-atom collisions, it is appropriate to apply the single-center close-coupling approach for the processes that cause predominantly direct excitations or involve

antiproton projectiles. In the single-center close-coupling approach, the heavy-particle motion assumed to be along a rectilinear straight-line trajectory $\mathbf{R}=\mathbf{b}+\mathbf{\upsilon}t$ with constant velocity, where b is the impact parameter. The assumption of a rectilinear trajectory implies that the incoming particle distinguishable from the target particles so that the effects of nuclear identity for proton collisions are neglected. The total wavefunction may be expanded in a complete set of the target states. Putting this expansion into the time-dependent Schrodinger equation describing the collision system leads to a set of coupled first-order differential equations for the expansion coefficients $c_n(b,\upsilon;z)$, where $z=\upsilon t$, (in atomic units) [3],

$$i\frac{\partial}{\partial z}c_n(b,\upsilon;z)=\frac{1}{\upsilon}\sum_k c_k(b,\upsilon;z)V_{nk}(\mathbf{R})\exp\left[-\frac{i}{\upsilon}(\varepsilon_k-\varepsilon_n)z\right],\qquad(1)$$

This set of equations is solved subject to the boundary condition that long before the collision, the expansion coefficient for the initial state wavefunction is unity and all other coefficients are zeros, i.e. $c_n(b,\upsilon;-\infty)=\delta_{0n}$.

The potential matrix elements $V_{nk}(\mathbf{R})$ are defined as

$$V_{nk}(\mathbf{R})=\int\varphi_n^*(\mathbf{r})V(\mathbf{r},\mathbf{R})\varphi_k(\mathbf{r})d\mathbf{r}.\qquad(2)$$

where the non-diagonal elements cause the transition, and the diagonal ones distort the wavelength of the rectilinear motion.

For the collision of a bare projectile ion (of charge Z_p) and a one-electron target (of nucleus charge Z_T), the time dependent projectile-target interaction is given by $V(\mathbf{r},\mathbf{R})=Z_p[Z_T/R-1/|\mathbf{R}-\mathbf{r}|]$. The eigenstates $\varphi_n(\mathbf{r})$ and the corresponding eigenenergies

ε_n of the target atom in the state $n \equiv (n,l,m)$ are defined as (see Ref. [25])

$$\phi_{nlm}(\mathbf{r}) = \sqrt{\left(\frac{2Z_T}{n}\right)^3 \frac{(n-l-1)!}{2n(n+l)!}} \left(\frac{2Z_T}{n}r\right)^l \exp\left[-\frac{Z_T r}{n}\right] L_{n+l}^{2l+1}\left(\frac{2Z_T}{n}r\right) Y_l^m(\hat{\mathbf{r}}), \qquad (3a)$$

$$\varepsilon_n = -\frac{Z_T^2}{2n^2}, \qquad (3b)$$

where $Y_l^m(\hat{\mathbf{r}})$ are the spherical harmonics and $L_\alpha^\beta(x)$ are Laguerre polynomials. The vector $\mathbf{r} \equiv \{r, \vartheta, \phi\}$ is the position vector of the electron, in the target atom, relative to the nucleus. Expanding the second term of $V(\mathbf{r},\mathbf{R})$ in spherical harmonics (see Ref. [26]) leads to analytical expressions for the matrix potential elements $V_{nk}(\mathbf{R})$ in terms of the incomplete Gamma functions and Clebsch-Gordan coefficients.

The primary quantities of interest are the cross sections for producing various final states of the system for given initial states of the target. The probability that the target will be in the final state n after the collision for a fixed impact parameter b is then given by $|c_n(b,\upsilon;+\infty)|^2$, and the total excitation cross section, which is in fact the experimentally measured quantity, is given by

$$\sigma_n = 2 \int_0^\infty |c_n(b,\upsilon;+\infty)|^2 \, b \, db \qquad (\pi a_0^2) \qquad (4)$$

where a_0^2 is the area of the first Bohr orbit of hydrogen and $\pi a_0^2 = 8.797 \times 10^{-17} \text{ cm}^2$.

In general, the Born series corresponding to the coupled equations (1) can be generated from the sequence of functions $c_n^{(j)}(b,\upsilon;z)$ satisfying:

$$c_n^{(j+1)}(b,\upsilon;z) = \delta_{n,0} - \frac{i}{\upsilon}\sum_{k}\int_{-\infty}^{z}dz' c_k^{(j)}(b,\upsilon;z')V_{nk}(\mathbf{R'})\exp[-\frac{i}{\upsilon}\omega_{kn}z'] \tag{5}$$

with $c_n^{(0)} = \delta_{n,0}$. The transition amplitude in the j-th Born approximation is $c_n^{(j)}$.

3. Results and discussion

In the present work, we investigate the 3s, 3p, and 3d direct excitations of Helium He$^+$(2s) and Lithium Li^{++}(2s) ions in collisions with protons or antiprotons. To understand the target charge effect on the excitation processes, it is convenient to calculate the scaled cross sections (for which the cross sections are multiplied by Z_T^4 [16]). The collision kinematics is described in the lab frame, where the target atom is assumed to be initially at rest and the collision energy is the kinetic energy of the projectile when it is far from the target prior to the collision (the incident energy of proton or antiproton projectile is $25\upsilon^2 Z_T^2$ keV).

The calculations are performed according to: (i) Numerical solution of the coupled differential equations (1) for different impact parameters by using the Bulirsch-Stoer method [27] which automatically adjusts the smallest step size of integration and save the time of calculations. It is found that the integration range $-1000 \leq z \leq 1000$ a. u. is sufficient where larger ranges give negligible changes in the results. We consider calculations take into account couplings between the n = 1, 2, 3, and 4 states of the target atom, cc n=4 states calculations, and others allow couplings to the higher excited states n=5 of the target atom, cc n=5 states calculations. The accuracy of the calculations can be enhanced by using a suitable substitution to pull out the oscillating factor $\exp[-i(\varepsilon_k - \varepsilon_n)z/\upsilon]$ from (1). It is

found that the integral (4) converges faster as the charge of the ionic nucleus increases or/and the incident energy decreases. (ii) Application of the usual second Born approximation, $c_n^{(2)}$, which allows for the possibility that the transition from an initial state 0 to the final state n may occur through sequence of virtual transitions via the other states. The second Born correction term is especially important if the $0 \rightarrow n$ is a weak transition and if there is a state *k* such that $0 \rightarrow k$ and $k \rightarrow n$ are strong transitions. In contrast, if $0 \rightarrow n$ is a strong transition the correction term is likely to be unimportant. (iii) Using the simplified formula of the second Born approximation in which the effect of all states other than the initial and the final states are neglected. This allows for the effect of the distortion in the initial and final states.

In the second Born calculations, the double integral is performed numerically by using Gauss-Legendre method [27], in polar coordinates, and the cross sections could only be calculated consistently to third order in the interaction potential [28], that is,

$$\left| c_n^{(2)} \right|^2 = \left| c_n^{(1)} \right|^2 \left\{ 1 + 2\operatorname{Re}\left(c_n^{(2)} / c_n^{(1)} - 1 \right) \right\} \tag{6}$$

Finally, for high-energy region comparison, we employ the first Born approximation (FBA) in the impact parameter formalism, $c_n^{(1)}$. It considers the direct transition to the final state only and neglects couplings between and to the other states.

As we see the approximations under consideration have different transition mechanisms enabling the final state to be reached indirectly through intermediate states.

In the following, the scaled cross sections for direct excitations of He$^+$(2s) and Li^{++}(2s) atoms in collisions with proton and antiproton are plotted against the scaled impact

energy $E_s = E/Z_T^2$. It is more convenient to denote to the present results of the same approximation in all processes by the same symbol. The cc n=5 states calculations are represented by curves a5 (b5) for proton (antiproton) impacts, while curves a4 (b4) represent the cc n=4 states calculations. Curves a2 (b2) and a3 (b3) refer to the results of the usual and simplified second-order Born calculations respectively, for proton (antiproton) projectiles. Curves b, for the first-order Born approximation which gives the same results for both proton and antiproton projectiles.

The present results for excitation of He$^+$(2s) and Li^{++}(2s) ions by proton impact are compared with the calculations of Ref. [11] (curves c) and Ref. [12] (curves d) respectively.

Figure 1 displays the 3s scaled cross sections of He$^+$(2s) target ion by proton (left panel) and antiproton (right panel) projectiles against the scaled impact energy E_s. It is found that the contribution of the second Born correction term, $c_n^{(2)} - c_n^{(1)}$, plays a different role in both proton and antiproton scattering processes. For proton impact, the usual second-order Born calculations (curve a2) bring the cross sections above those of the first-order Born results (curve b) in the whole energy region, while the simplified second-order Born calculations (curve a3) reduce the cross sections below the first-order Born results at impact energies above 4 keV. The situation is changed in the case of antiproton-induced reactions with some difference in the magnitude. Therefore, we can say that the mechanism of the electronic transitions allowed by each of the usual and simplified second-order Born approximations is strongly affected by the sign of the projectile charge.

Curves a5 (b5) for the results of the cc n=5 states approximation for proton (antiproton) and the corresponding results of the cc n=4 states approximation (curves a4

(b4)) show the different influence, of including couplings to and between the higher excited states n=5 of the target ion, on both of the proton- and antiproton-induced reactions. It is clear that allowing couplings to and between n=5 states of the target ion enhances the 3s scaled cross sections for proton impact, while an opposite situation takes place for the antiproton one.

The percent deviations, of the excitation cross sections of He+ by proton (antiproton) impact, obtained by the cc n=5 states calculations from those obtained by the cc n=4 states calculations are given in table 1 (2). This allows one to gauge the accuracy of convergence of the calculations for a particular transition. It is found that the highest percent deviation of the cc n= 5 states calculations from those of the cc n=4 states calculations is about 20% around 3.75 keV scaled impact energy for proton projectile and it is about -50% around 2 keV scaled impact energy for antiproton projectile.

The simplified second-order Born calculations for proton projectile (curve a3) is in excellent agreement with the calculations of Hall et al. [11] (curve c), while the other present calculations converge to the calculations of Hall et al. [11] at energies above 150 keV.

At high impact energies, the simplified second-order Born cross sections for antiproton projectile (curve b3) converges to the first-order Born calculations (curve b) from above while the other calculations do from below. The situation is completely changed for the results due to proton projectile.

The 3s scaled cross sections of $Li^{++}(2s)$ target ions by protons (left panel) and antiprotons (right panel) impacts are shown in figure 2. It is clear that the cross section peaks appeared in figure 1 for He^+ target ion still take place for the cross sections of the

Li^{++} target ion, in figure 2, but they are shifted to higher impact energies and with fewer magnitudes. It is found that the contribution of the correction term in the second-order Born approximations affects on the cross sections of both He^{+} and Li^{++} target ions in a similar way, but with the different order of magnitude. In figure 2, the low energy maximum peak of the simplified second-Born cross section (curve a3) for proton-induced reaction and the maximum peak of the usual second-Born cross section (curve b2) for antiproton-induced reaction become much lower than that of the first-order Born approximation (curves b).

The results of the present coupled-state calculations show that involving the n=5 states of the target ion increases the cross sections in the case of proton projectile. The same applies for the antiproton-induced reaction at energies less than 10 keV. However, the effect of allowing couplings to and between n=5 states of the target ion on the 3s cross section of Li^{++} target ion is smaller than it in the case of He+ target ion.

The percent deviations, of the excitation cross sections of Li^{++} by proton (antiproton) impact, obtained by the cc n=5 states calculations from those obtained by the cc n=4 states calculations are given in table 3 (4). It is found that the highest percent deviation is about 30% around 4.5 keV impact energy for proton projectile and it is about 15% around 5.6 keV impact energy for antiproton projectile.

The low-energy behavior of the 3s-cross sections due to the Li^{++} target ion (fig. 2) is different from those due to the He^{+} target ion (figure 1), especially in the case of proton projectiles. At high impact energies, the cross sections converge to the first-order Born calculations (curve b) in a similar way as the case of He^{+} target ion but at higher impact energies. This maybe due to increasing the velocity of the ionic electron with increasing the

charge of the ionic nucleus. The oscillatory behavior shown by curves a5, a4, and a3 for both He+ target ion (figure 1) and Li^{++} target ion (figure 2) at low and intermediate energies reveals the importance of the influence of the capture probability of the electron by the incident proton, which is not allowed in the case of the antiproton scattering processes, in the mechanisms of these approximations.

It is clear that both of the coupled-state calculations (curves a5 and a4) and the first-order Born calculations (curve b) improve the agreement with the calculations of Hall et al. [12] (curve d).

Figure 3 illustrates the 3p scaled excitation cross sections of He^{+} (2s) ion due to the interaction with protons (left panel) and antiprotons (right panel). It is found that the results due to antiproton-induced reactions, for all the approximations under consideration, are greater than those due to proton-induced reactions except for the coupled-state calculations at energies below 16 keV. It is seen that the effect of the second Born correction term on the simplified second-order Born calculations is much greater than it on the usual second-order Born calculations. The usual second-order approximation increases the cross sections in the case of antiproton impact in the whole energy range while an opposite situation takes place in the case of proton impact at energies above 15 keV. We can also see that the simplified second-order Born approximation reduces the cross sections in the case of proton impact in the energy region $7<E_s<60$ keV, and those due to the antiproton impact at energies above 60 keV.

The curves in Fig. 3 show that involving the n=5 states of the He^{+} ion reduces the cross sections due to antiproton impact and has the negligible effect at energies above 14 keV. An opposite situation occurs for proton projectile at energies below 30 keV. It is seen

12

that the effect of the projectile charge on the coupled-state calculations is the strongest one, especially at low impact energies. Also, we can note that the coupled-state calculations (curves a4 and a5) improve the comparison with the calculations of Hall et al. [11] (curve c).

The percent deviations, of the scaled cross sections obtained by the cc n=5 states calculations from those obtained by the cc n=4 states calculations in tables 1 and 2 show that the highest percent deviation in the case of He+ ion is about 29% at 2 keV impact energy for proton projectile and it is about -33% around 3.75 keV impact energy for antiproton projectile.

At high energies, the simplified second-order Born calculations for the both projectiles (curves a3 and b3) converge to the first-order Born calculations (curve b) at energies much earlier than the results of the other calculations. However, the usual second-order Born calculations for antiproton (curve b2) and the simplified second-order Born calculations (curve a3), for proton impact, converge to the first-order Born calculations from above while the others do from below.

The 3p excitation cross sections of $Li^{++}(2s)$ ions by collisions with the proton (left panel) and antiproton (right panel) are plotted in figure 4. We can see that the effect of each of the

second Born correction term and allowing couplings to and between n=5 states of the Li^{++} target ion are somewhat similar to, but smaller than, that in the case of the He^+ target ion (figure 3). The effect of considering couplings to and between n=5 states of the Li^{++} target ion, on the antiproton results is much greater than it on the proton ones.

From tables 3 and 4 we can see that highest percent deviation in the case of Li$^+$ ion is about 19% for proton projectile around 5.6 keV impact energy and it is about -25% for antiproton projectile around 9 keV impact energy. It is seen that the coupled-state calculations (curves a4 and a5) are in excellent agreement with the calculations of Hall et al. [12] (curve c).

The curves in figures 3 and 4 show that the low-energy dependence of the 3p cross sections of both target ions are quite different. Convergence of the different calculations to the first-order Born calculations (curve b), at high energies, occurs in a similar way for both targets, but at higher energies in the case of Li^{++} target ion.

The 3d scaled cross sections for scattering processes of proton (left panel) and antiproton (right panel) by He$^+$(2s) and Li^{++}(2s) ions are demonstrated in figures 5 and 6, respectively. It is found that the effect of the projectile charge on the simplified second-order Born calculations is the weakest. We can see that the second Born correction term in the simplified second-order Born approximation enhances the cross sections for both targets and projectiles except for the antiproton impact at impact energies greater than 15 keV in the case of He$^+$ ion and at energies greater than 25 keV in the case of Li^{++} ion. However, the contribution of the correction term on the simplified second-order Born calculations is much greater than it in the usual second–order Born calculations.

At low impact energies, in contrast to the 3s and 3p excitation processes, the 3d excitation cross section of both He$^+$ and Li^{++} ions have a similar behavior for both projectiles except the usual second-order Born calculations (a2) for and Li^{++} ion, and do not show the oscillatory structure. Curves a3 and b3 in figures 5 and 6 show that the simplified second-order Born calculations converge to those of the first-order Born approximation (curve b) at

energies much higher than the other calculations. This may be referred to the importance of the couplings neglected by this approximation in the $2s \rightarrow 3d$ transitions.

A comparison between the present cc n=4 and cc n=5 states calculations demonstrates that extending the couples-state calculations to include n=5 states of the target ions reduces the cross sections due to the antiproton-induced reactions and increases, by smaller amounts, those due to the proton ones. The percent deviations, of the scaled cross sections obtained by the cc n=5 states calculations from those obtained by the cc n=4 states calculations in tables 1 and 2 show that the highest percent deviation in the case of He^+ ion is about 20% at 2 keV impact energy for proton projectile and it is about -28% around 7.5 keV impact energy for antiproton projectile. From tables 3 and 4 we can also see that highest percent deviation in the case of Li^+ ion is about 12% for proton projectile and it is about -21% for antiproton projectile around 9 keV impact energy.

From figures 1-6, it is easy to notice that the effect of the projectile charge on the 3d cross sections is much weaker than it in the 3s or 3p cross sections.

It is obvious that the coupled-state calculations for proton projectile (curves a4 and a5) improve the comparison with the calculations by Hall et al. [11] for He^+ target ion (curve c) and Hall et al. [12] for Li^{++} target ion (curve d).

Finally, we can report that the contribution of the second Born correction term in each of the simplified and usual second-order Born approximations, for both proton and antiproton-induced reactions, varied from one channel to another. In general, the tendency of sequences of transitions is to strengthen weak transitions and weaken strong transitions. Increasing the charge of the target nucleus increases leads to weak interaction between the

electron of the target and the projectile, and reduces the excitation cross sections. In general, allowing coupling to and between n=5 states of the target ion enhances the cross sections for proton projectile and reduces it to the antiproton one. This may be expected because of including higher excited states of the target ion increases the probability of the electron-exchange in the case of proton scattering process. It is found that the cross sections for antiprotons cross those for protons, at low and intermediate energies. This may be attributed to the so-called binding/antibinding effect in the close collisions that dominate excitation at low velocities. The convergence of the results of the different approximations to those of the first-order Born approximation at high energies is confirmed, where the high energy region is shifted to the higher domain as the charge of the ionic nucleus increases, this may be due to increasing the velocity of the ionic electron.

4. Conclusion

The scaled excitation cross sections of $He^+(2s)$ and $Li^{++}(2s)$ ions by protons or antiprotons impacts have been investigated in the framework of a one-center atomic-orbital close-coupling method as well as the impact parameter versions of the first- and second-order Born approximations. It is seen that the contribution of the second Born correction term, to the calculations, in each of the usual and simplified second-order Born approximations is affected by the charge of the projectile much greater than it by the charge of the ionic nucleus. The calculations showed that the energy-dependence of the cross sections is strongly affected by the possible electronic transitions allowed by the used approximations. Including higher excited states, n=5, of the target ions affects on the antiproton cross sections greater than the proton ones. Increasing the binding energy, as the charge of the target nucleus increases, leads to a small electron capture probability in

16

the case of the proton. Therefore the effect of the sign of the projectile charge decreases as the charge of the ionic nucleus increases.

References

[1] T.G. Winter. Adv. At. Mol. Opt. Phys., **52**, 391 (2005).

[2] J.S. Cohen. Rep. Prog., Phys., 67, 1769 (2004).

[3] W. Fritsch and C.D. Lin. Phys. Rep., **202**, 1 (1991).

[4] C.D. Lin, Review of Fundamental Processes and Application of Atoms and Ions (World Scientific, Singapore. 1993).

[5] B.H. Bransden, *Atomic Collision Theory* (Benjamin-Cummings, Reading. 1983).

[6] H. Knudsen, U. Mikkelsen, K. Paludan, K. Kirsbom, S.P. Møller, E. Uggerhøj, J. Slevin, M. Charlton, and E. Morenzoni, Phys. Rev. Lett., **74**, 4627 (1995).

[7] T. Watanabe, X.M. Tong, D. Kato, and S. Ohtani, J. Chin. Chem. Soc., **48**, 505 (2001).

[8] B. Manaut, S. Taj, and M. El Idrissi, Can. J. Phys., **91**, 696 (2013).

[9] C.O. Reinhold, R. E. Olson, and W. Fritsch, Phys. Rev. A, **41**, 4837 (1990).

[10] A.L. Ford, J.F. Reading, and K.A. Hall, J. Phys. B: At. Mol. Opt. Phys. 26, 4537 (1993).

[11] K.A. Hall, J.F. Reading, and A.L. Ford, J. Phys. B: At. Mol. Opt. Phys., **27**, 5257 (1994).

[12] K.A. Hall, J.F. Reading, and A.L. Ford, J. Phys. B: At. Mol. Opt. Phys., **29**, 1979 (1996).

[13] X. Tong, D. Kato, T. Watanabe, and S. Ohtani, J. Phys. B: At. Mol. Opt. Phys., **33** 5585 (2000).

[14] X. Tong, T. Watanabe, D. Kato, and S. Ohtani, Phys. Rev. A, **66**, 032708 (2002).

[15] A.V. Nefiodov and G. Plunien, J. Phys. B: At. Mol. Opt. Phys., 43, 165206 (2010).

[16] T.G. Winter, Phys. Rev. A , **87**, 032704 (2013).

[17] B. Najjari and A.B. Voitkiv, Phys. Rev. A, **87**, 034701 (2013).

[18] F. Khelfaoui, B. Lasri, and O. Abbes, J. Mater. Sc. and En. A, **3**, 66 (2013).

[19] D.R. Schultz, J.C. Wells, P.S. Krstic, and C.O. Reinhold, Phys. Rev. A, 56, 3710 (1997).

[20] L. Liu, J.G. Wang, and R.K. Janev, J. Phys. B: At. Mol. Opt. Phys., **42**, 105206 (2009).

[21] E. Gusarevich and V. Matveev, J. of Exp. and Theo. Phys., **107**, 933 (2008).

[22] R.S. Tantawi, Chin. Phys. Lett., 20, 366 (2003).

[23] R.S. Tantawi, J. Korean Phys. Soc., **64**, 382 (2014).

[24] R.S. Tantawi and A. Nagah, Can. J. of Phys. 10.1139/cjp-2015-0045.

[25] L. Schiff, *Quantum mechanics* (McGraw Hill, New York. 1968).

[26] P. G. Burke and C. J. Joachain, *Theory of Electron-Atom Collisions: Part 1: Potential Scattering* (Plenum Press, New York 1995)

[27] W.H. Press, S.A. Teukolsky, W.T. Vetterling, and B.P. Flannery, *Numerical recipes* (Cambridge University Press, New York. 1992).

[28] A.E. Kingston, B.L. Moiseiwitsch, and B.G. Skinner, Proc. R. Soc. London, Ser. A, 258, 237 (1960).

Figures caption

Figure 1. The 3s scaled cross sections for direct excitation of He$^+$(2s) ions by proton (left panel) and antiproton (right panel) projectiles as functions of the scaled impact energy E_s. Present work: (b) first-order Born calculations; a5 (b5), close-coupling calculations taking into account couplings between n=1-5 states of the target ion; a4 (b4), close-coupling calculations considering couplings between n=1-4 states of the target ion; a2 (b2), usual second-order Born calculations; and a3 (b3) simplified second-order Born calculations, for proton (antiproton) impacts. Previous work: c is taken from Ref. 11 for proton collision.

Figure 2. The 3s scaled cross sections for direct excitation of Li^{++}(2s) ions by proton (left panel) and antiproton (right panel) projectiles as functions of the scaled impact energy E_s. Present work: (b) first-order Born calculations; a5 (b5), close-coupling calculations taking into account couplings between n=1-5 states of the target ion; a4 (b4), close-coupling calculations considering couplings between n=1-4 states of the target ion; a2 (b2), usual second-order Born calculations; and a3 (b3) simplified second-order Born calculations, for proton (antiproton) impacts. Previous work: d is taken from Ref. 12 for proton collision.

Figure 3. The same as figure 1 but for 3p-scaled cross sections.

Figure 4. The same as figure 2 but for 3p- scaled cross sections.

Figure 5. The same as figure 1 but for 3d- scaled cross sections.

Figure 6. The same as figure 2 but for 3d- scaled cross sections.

Tables caption

Table 1. The percent deviations, of the excitation scaled cross sections of He$^+$ by proton impact, obtained by the cc n=5 states calculations from those obtained by the cc n=4 states calculations.

Table 2. The percent deviations, of the excitation scaled cross sections of He$^+$ by antiproton impact, obtained by the cc n=5 states calculations from those obtained by the cc n=4 states calculations.

**Table 3**. The percent deviations, of the excitation scaled cross sections of Li^{++} by proton impact, obtained by the cc n=5 states calculations from those obtained by the cc n=4 states calculations.

Table 4. The percent deviations, of the excitation scaled cross sections of Li^{++} by antiproton impact, obtained by the cc n=5 states calculations from those obtained by the cc n=4 states calculations.
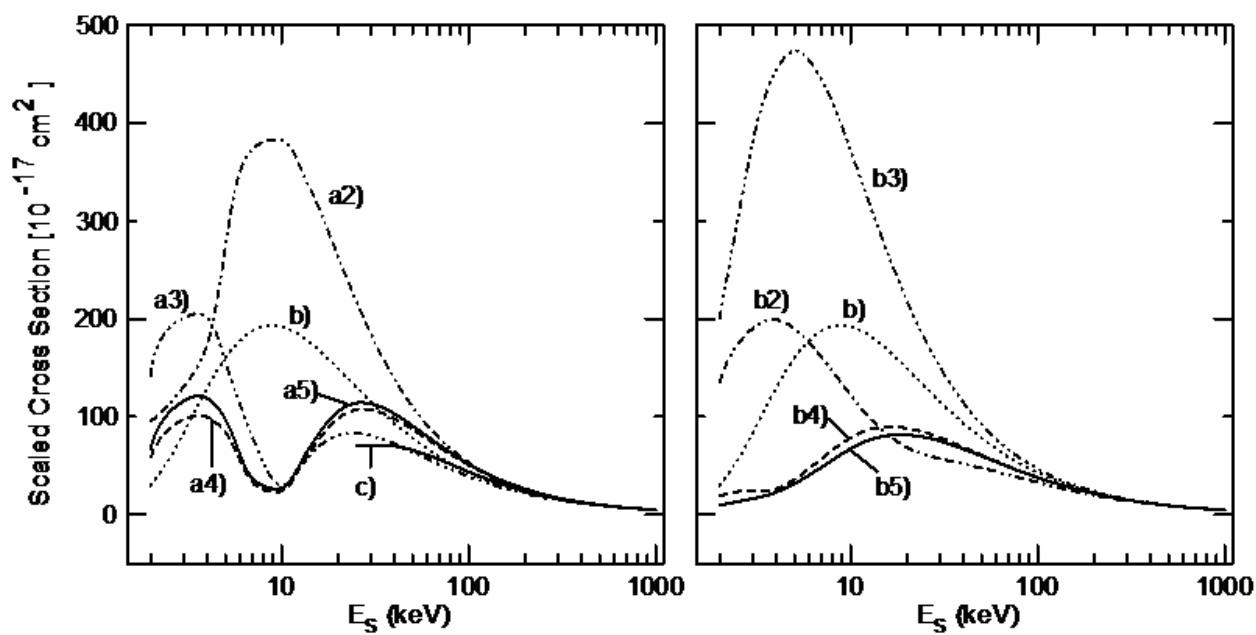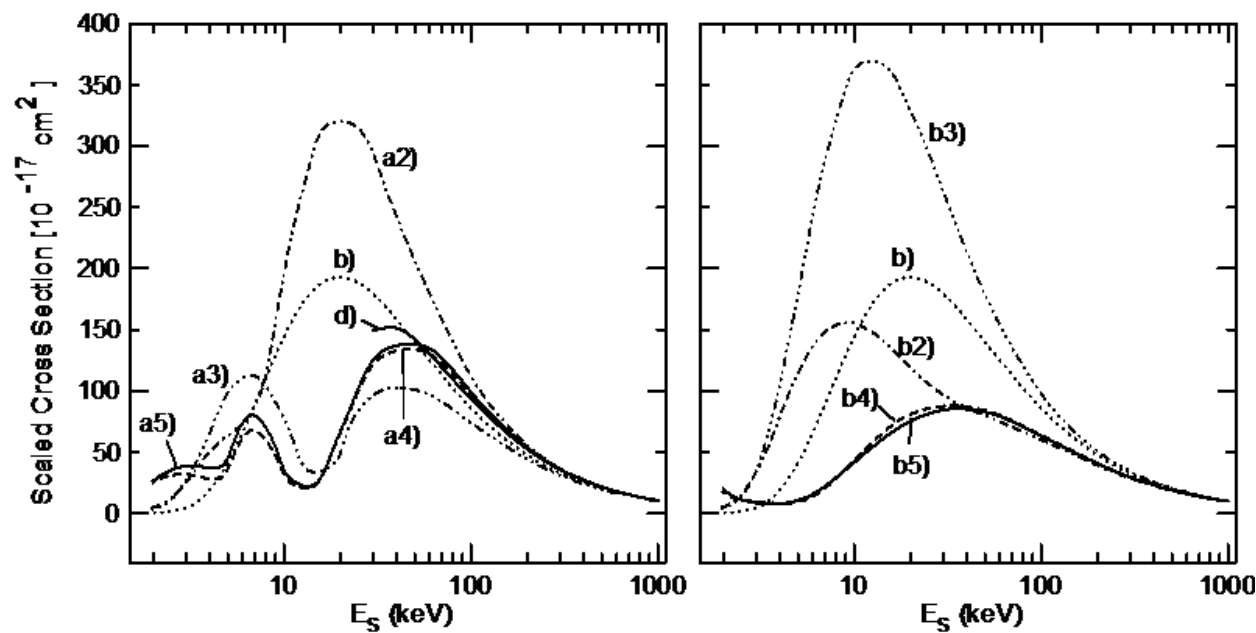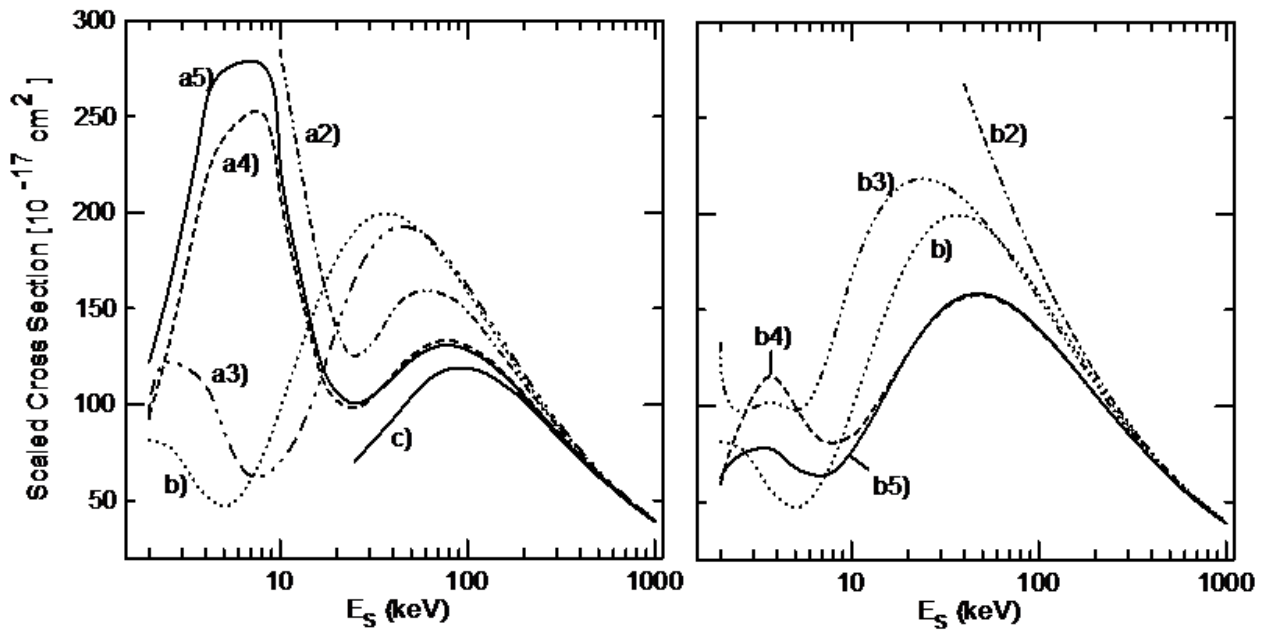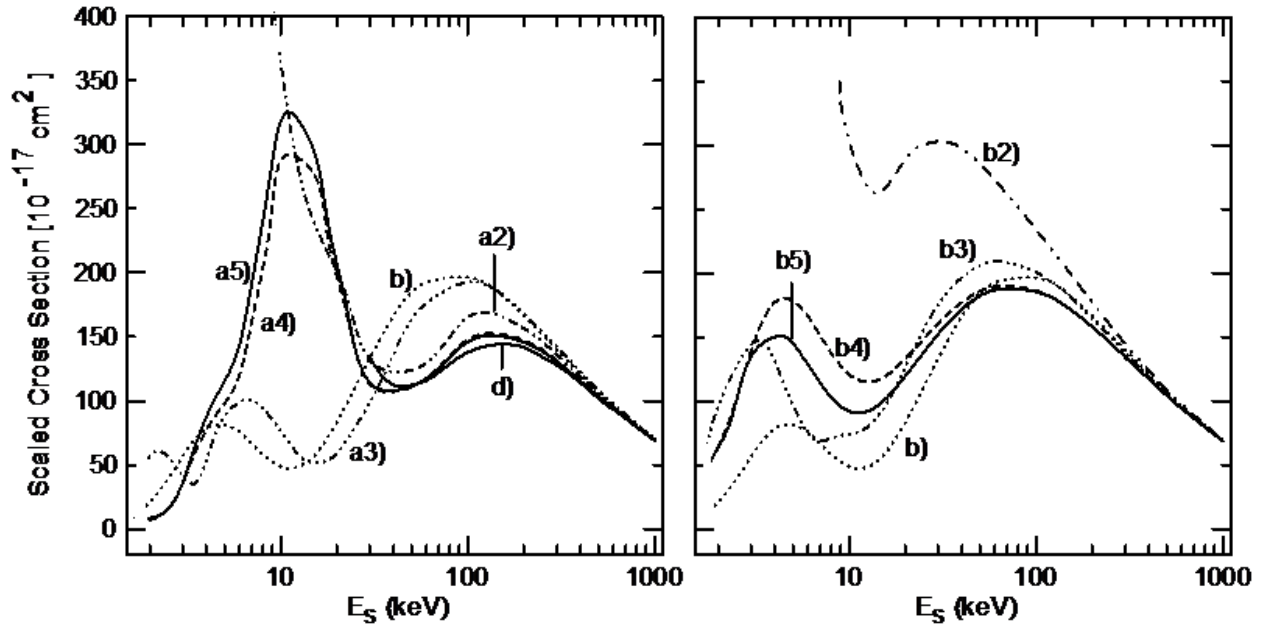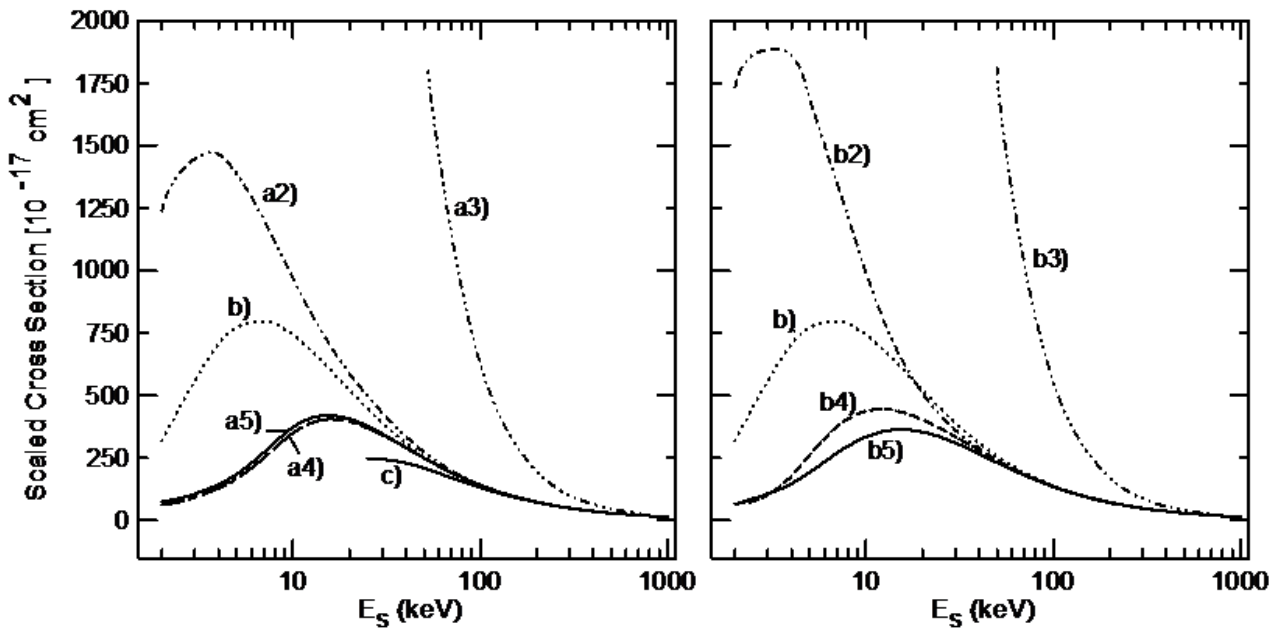
Figure 1

Figure 2

22

Figure 3

Figure 4

Figure 5
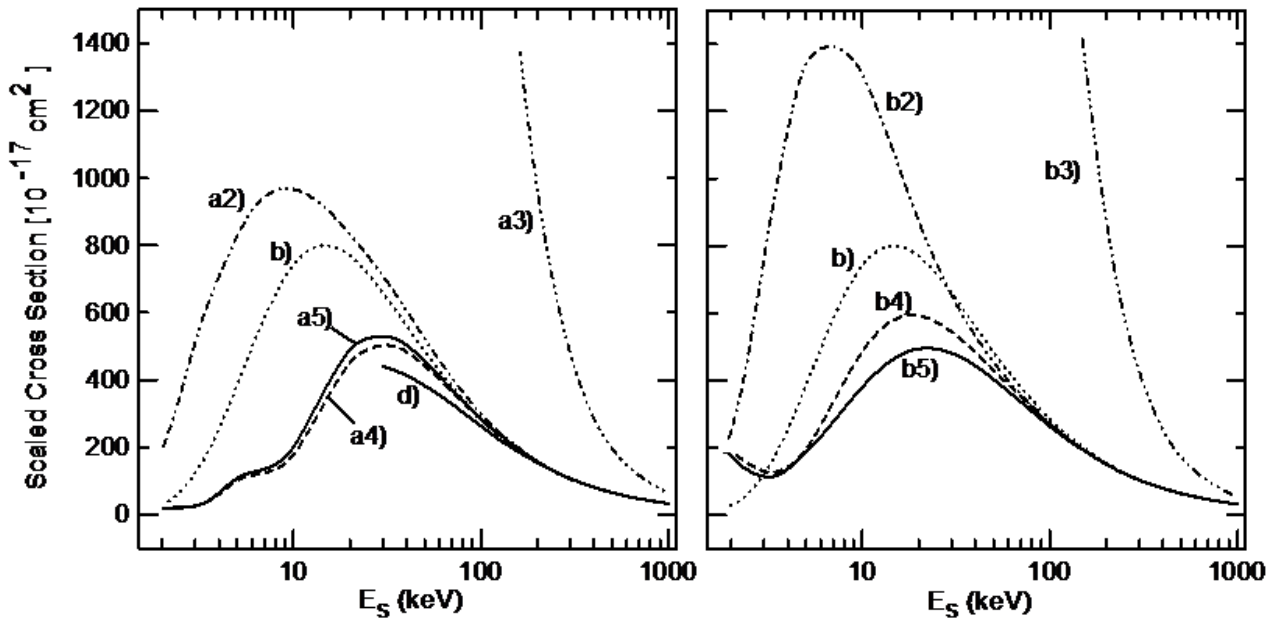
Figure 6

Table 1.

$\backslash E_s$ (keV)	2	3.75	7.5	15	25	50	250
2s→3s	15%	20%	14.5%	8%	4%	4%	0.2%
2s→3p	29%	17%	10%	5%	2.6%	-1.7%	-0.8%
2s→3d	20%	12%	8%	4%	1.8%	0.4%	0.05%

Table 2.

$\backslash E_s(\text{keV})$	2	3.75	7.5	15	25	50	250
2s→3s	-50%	-15%	-15%	-11%	-6%	-1.3%	-0.3%
2s→3p	6%	-33%	-20%	-2%	0.3%	0.6%	0.3%
2s→3d	-4.3%	-13%	-28%	-17%	-9%	-3%	-0.01%

Table 3.

$\backslash E_s(\text{keV})$	2.2	5.6	9	14	33	110	222
2s→3s	8.6%	23%	15%	5%	3%	1.7%	0.5%
2s→3p	7%	19%	15%	8%	1%	-1%	-0.9%
2s→3d	9.7%	7%	12%	11%	5%	0.8%	0.2%

Table 4.

$\backslash E_s(\text{keV})$	2.2	5.6	9	14	33	110	222
2s→3s	7.5%	15%	-0.6%	-7%	-3%	-1%	-0.08%
2s→3p	-4%	-21%	-25%	-18%	-4%	-0.2%	-0.2%
2s→3d	-12%	-9.5%	-21%	-20%	-10%	-2%	-0.6%